



### IIR FILTER

To suppress the mechanical modes of the piezo system, the IIR filter with a difference equation as shown in (1), is applied in the tuner feedback system. It is a simple IIR filter with only one real pole. The filter bandwidth is proportional to the adjustable parameter  $\alpha$ .

$$y(n) = \alpha \cdot x(n) + (1 - \alpha) \cdot y(n-1), \quad \alpha \ll 1 \quad (1)$$

The realization of the IIR filter in the previous tuner system is shown in Fig. 3(a). This IIR filter works well if the filter bandwidth is large enough (e.g.  $f_{BW} \geq 1$  kHz). However, in the low-bandwidth case, the finite word length (FWL) effects produce a significant degradation of the filtering characteristics. To decrease the FWL effects, we have to increase the bit sizes of the two  $18 \times 24$  multipliers in Fig. 3(a). As a result, the DSP hardware resources inside FPGA also have to be increased. Since that type of IIR filters are widely used in the digital LLRF systems and tuner systems in cERL, it is worthwhile to optimize the structure of this filter.

After a simple transformation, the difference equation in (1) can be transformed to (2). The corresponding realization of (2) is presented in Fig. 3(b). It can be clearly observed that the proposed structure requires only one  $24 \times 36$  multiplier. Therefore, additional DSP hardware resources are not necessary even if the bits of the multiplier are doubled.

$$y(n) = \alpha \cdot [x(n) - y(n-1)] + y(n-1), \quad \alpha \ll 1 \quad (2)$$

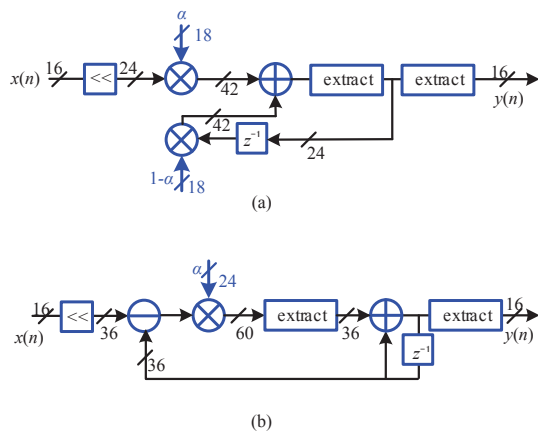


Figure 3: Realization of the previous (a) and proposed (b) IIR filter of the tuner system.

### DOB CONTROL OF TUNER SYSTEM

DOB control is an advanced control approach that aims at rejecting the disturbances in a control system. Since there are various disturbances in both the LLRF and tuner systems, the DOB control can be a suitable approach for these control issues. We have already implemented the DOB-based control method in the LLRF system in the cERL commissioning successfully [5-7], hence, we would like to apply this method in the tuner system also.

According to the basics of the DOB approach presented in [5-7], a nominal open-loop system model is required for the DOB control. The complete mathematical model (transfer function) of the tuner system is given in [9]

$$H(s) = \left( \frac{M_0}{\tau s + 1} + \sum_{k=1}^N \frac{\omega_k^2 M_k}{s^2 + 2\xi_k \omega_k s + \omega_k^2} \right) e^{-T_d s} \quad (3)$$

The parameter  $T_d$  outside the parentheses in (3) represents the measured group delay. The first-order components in the parentheses represent the passband of the tuner system, where  $M_0$  is the steady state gain and  $\tau$  a low-pass time constant. The second-order components are related to the high-frequency modes. Owing to the very tight time schedule in the cERL beam commissioning, we didn't have enough time to identify the detailed high-frequency modes of the tuner system, i.e., the coefficients of the second order component in (3). In this paper, we considered a tuner system of a first-order model with group delay that can be expressed by

$$H_n(s) = \frac{M_0}{\tau s + 1} e^{-T_d s} \quad (4)$$

The coefficients in (4) were identified by exciting the tuner system with a square wave in the DAC output and measuring the response of the phase difference;  $\Delta\theta$  (see Fig. 4). After simple data analysis, the parameters such as group delay and time constant were obtained.

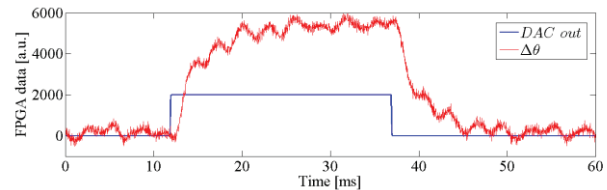


Figure 4: Simple identification experiment for the model in (4). Some high-frequency modes around 340 Hz can be also observed.

Similar to DOB control of the LLRF system [5-7], the overall model of the DOB control and previous integral individual control of the tuner system is shown in Fig. 5. The presented DOB-based controller is indicated by the red dotted rectangle. The switch "SW" in Fig. 5 controls the enable/disable operation of the DOB controller, and the parameter  $G_{DOB}$  regulates the gain of the DOB controller. The IIR filter in Fig. 3 (b) is applied in the digital filters of  $F_1(z)$ ,  $F_{ADC}(z)$  and  $F_{DAC}(z)$ . The bandwidths of both  $F_{ADC}(z)$  and  $F_{DAC}(z)$  are more than 5 kHz. The bandwidth of  $F_1(z)$  was set to be 25 Hz to suppress the 50 Hz components in ML cavities [6]. The definition of each model is summarized in Table I. In principle, the real disturbances  $d$  in the tuner system can be estimated by the DOB controller output,  $d_e$ , therefore, after removing that  $d_e$  in the tuner feedback loops, we can improve the disturbance rejection characteristics of the system [5-7].

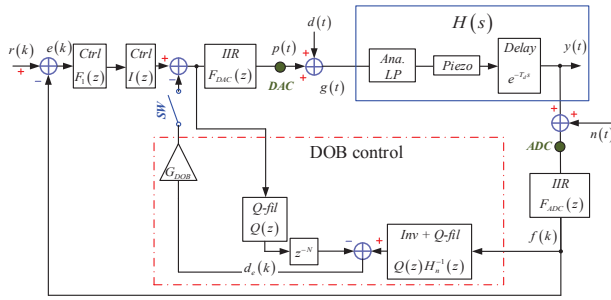


Figure 5: Overall model of “I+DOB” control, the DOB controller is indicated by the red dotted rectangles.

Table 1: Definition of the Models and Parameters in Fig. 5

Parameters	Definition
$d(t)$	Disturbance signal
$d_e(k)$	Estimated disturbance by DOB control
$y(t)$	Phase difference
$n(t)$	High frequency noise signal
$Q(z)$	Q-filter model, a second order IIR filter
$F_{1,ADC,DAC}(z)$	IIR filter presented in (2)
$z^{-N}$	Nominal group delay model
$G_{DOB}$	Gain of the DOB control (from 0 to 1)
$I(z)$	Integral controller
$H(s)$	Real open-loop model of tuner system
$H_n(z)$	Nominal open-loop model of tuner system (w/o group delay)

## EXPERIMENT ON CERL BEAM COMMISSIONING

We developed a DOB-based controller in an FPGA and demonstrated its performance in the digital tuner system of the ML cavities. Models (parameters) of the controllers used in the experiments are given in (5), (6) and (7). At first, we tried to operate the tuner system with integral individual control (by switching off the “SW” in Fig. 5), and we measured the phase differences;  $\Delta\theta$ . In the next step, we switched on the DOB control, gradually raised the DOB gain  $G_{DOB}$  from 0 to 1, and then measured the phase differences again. With increase in the  $G_{DOB}$ , the disturbances in the phase differences reduced; however, when the gain was raised to 0.5, the components around 340 Hz is excited and system became unstable (see Fig. 4 and Fig. 7). The most probable reason is that there is a mechanical mode around 340 Hz, which is excited by the inverse components  $H_n^{-1}(z)$  of the DOB controller (see Fig. 5).

$$H_n(s) = \frac{2.7}{0.0016 \cdot s + 1} e^{-0.0005 \cdot s} \quad (5)$$

$$Q(s) = \left( \frac{2\pi \cdot 1000}{s + 2\pi \cdot 1000} \right)^2 \quad (6)$$

$$I(s) = \frac{15.5}{s} \quad (7)$$

Figure 6 compares the measured phase differences (left: waveform, right: spectrum) of the integral individual control and “I+DOB” control. Here, the gain of the DOB control ( $G_{DOB}$ ) is 0.4 (the highest value we could successfully reach). It can be observed that, the disturbance in the low frequency domain (DC to 100 Hz) are rejected well by the DOB controller.

Figure 7 shows the 340 Hz component excited in the case of  $G_{DOB} = 0.5$ . It seems that the simple first-order model in (4) is not sufficient to represent the behavior of a real tuner system; thus, higher precision system identification is necessary.

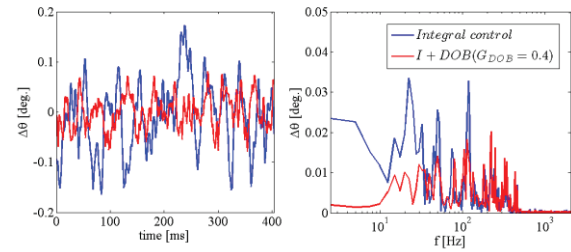


Figure 6: Integral individual control (blue) vs. “I+DOB” control (red). The waveform of phase difference (left) is plotted as well as its FFT analysis (right).

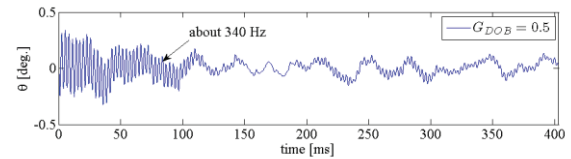


Figure 7: Tuner system becomes unstable in the case of  $G_{DOB} = 0.5$ . A component at approximately 340 Hz was excited.

## SUMMARY

Digital LLRF systems and tuner systems were developed for the cERL. To decrease the influence of the FWL effects of the tuner system, we first optimized the structure of the IIR filter. Furthermore, to improve the disturbance rejection, we implemented a DOB-based control approach for the tuner system. Experiments in beam commissioning indicated that the DOB control was effective in rejecting the low-frequency disturbances. However, due to the probable existence of mechanical modes, the gain of the DOB controller was limited to less than 0.5. A higher-precision system model is required for further improvement in the system performance.

**REFERENCES**

- [1] N. Nakamura et al., “Present status of the compact ERL at KEK,” Proc. IPAC2014, Dresden, Germany (2014).
- [2] S. Sakanaka et al., “Construction and commissioning of compact-ERL Injector at KEK,” Proc. ERL2013, Novosibirsk, Russia (2013).
- [3] T. Miura et al., “Performance of RF systems for compact ERL injector at KEK,” Proc. ERL 2013, Novosibirsk, Russia (2013).
- [4] T. Miura et al., “Performance of RF system for compact-ERL main linac at KEK,” Proc. IPAC’14, Dresden, Germany (2014).
- [5] F. Qiu et al., “A disturbance-observer-based controller for LLRF systems,” Proc. IPAC’15, Richmond, USA (2015).
- [6] F. Qiu et al., “Performance of the digital LLRF systems at KEK cERL,” Proc. ERL2015, New York, USA (2015).
- [7] F. Qiu et al., “Application of disturbance observer-based control in low-level radio-frequency system in a compact energy recovery linac at KEK,” PRSTAB 18, 092801(2015).
- [8] K. Enami et al., “Performance evaluation of ERL main linac tuner,” Proc. IPAC’14, Dresden, Germany (2014).
- [9] A. Neumann et al., “Analysis of active compensation of microphonics in continue wave narrow-bandwidth superconducting cavities,” PRSTAB 13, 082001 (2010).